

Compton Scattering

MIT Department of Physics

You will observe the scattering of 661.6 keV photons by electrons and measure the energies of the scattered gamma rays as well as the energies of the recoil electrons. The results can be compared with the formulas for Compton scattering, considering the quantized photon like a particle.

PREPARATORY QUESTIONS

Please visit the Compton Scattering chapter on the course website to review the background material for this experiment. Answer all questions found in the chapter. Work out the solutions in your laboratory notebook; submit your answers on the course website. [Note: Not available to OCW users]

SUGGESTED SCHEDULE

- Day 1: Familiarize yourself with the equipment and do Section III.1.
- Day 2: Repeat Section III.1 and do Section III.2. By the end of this session you should have verified that $E_{scat} + E_{recoil} \approx 662$ keV for at least two angular positions.
- Day 3: Perform Section III.3.
- Day 4: Repeat portions of the experiment that need improvement.

I. INTRODUCTION

By 1920 the successes of the quantum theories of black-body spectra (Planck, 1901), the photoelectric effect (Einstein, 1905) and the hydrogen spectrum (Bohr, 1913) had established the idea that interactions between electromagnetic radiation of frequency ν and matter occur through the emission or absorption of discrete quanta of energy $E = h\nu$. The next crucial step in the development of the modern concept of the photon as the particle of electromagnetic radiation was taken by Arthur Compton in the interpretation of experiments he initiated in 1920 to measure with precision the wavelengths of X-rays scattered from electrons in materials of (low atomic number) [1, 3]. The phenomena of X-ray scattering had already been studied intensively. It was known that the penetrating power of X-rays decreases with increasing wavelength and that X-rays are less penetrating after being scattered than before, which indicated that the scattering process somehow increases their wavelength.

Compton's idea was to use the recently developed technique of high-resolution X-ray spectrometry, based on measurement of the angle of Bragg reflection of X-rays from crystals, to measure precisely the wavelengths of the scattered X-rays [4]. Irradiating a carbon target with

an intense collimated beam of monochromatic molybdenum K_α X-rays and using an ionization chamber as the detector in his spectrometer, Compton found that the spectrum of scattered X-rays had two distinct spectral lines, one at the wavelength of the incident X-rays and another at a wavelength that was longer by an amount that depends on the angle of scattering. The scattering without a wavelength shift was readily explained by the classical theory of coherent scattering of electromagnetic waves from electrons bound in atoms. However, the classical theory provided no explanation of the wavelength-shifting "incoherent" scattering process. The phenomenon of Bragg reflection used in Compton's measurements was a clear demonstration of the wavelike character of the X-rays. Nevertheless, Compton put forward the apparently contradictory idea that X-rays, known to be electromagnetic radiation of very short wavelength, interact with electrons like particles of zero rest mass so that their energy $E = h\nu = hc/\lambda$ and momentum p are related by the relativistic equation for particles of zero rest mass, namely $p = E/c$. He calculated according to relativistic mechanics the relations between the initial and final energies and momenta of an X-ray quantum and a free electron involved, like billiard balls, in an elastic collision. In this way he arrived at the formula for the "Compton shift" in the wavelength of incoherently scattered X-rays, namely (see [2], Appendix A)

$$\Delta\lambda = \frac{h}{mc}(1 - \cos\theta), \quad (1)$$

where m is the mass of the electron and θ is the angle between the trajectories of the incident and scattered photon.

The agreement between Compton's experimental results confronted physicists and philosophers with the conceptual dilemma of the particle-wave duality of electromagnetic radiation. In particular, how was one to understand how each particle of light in a Young interference experiment goes simultaneously through two slits? The dilemma was further compounded when, in 1924, de Broglie put forward the idea that material particles (*i.e.* electrons, protons, atoms, etc.) should exhibit wave-like properties characterized by a wavelength λ related to their momentum p by the same formula as that for light quanta, namely $\lambda = h/p$. In 1927 the wave-like properties of electrons were discovered by Davisson and Germer in experiments on the reflection of electrons from crystals. A particularly interesting account of these developments is given by Compton and Allison in their classic treatise [5].

I.1. Experimental Goals

In this experiment you will measure:

1. the energies of Compton-scattered gamma-ray photons and recoil electrons,
2. the frequency of scattering as a function of angle θ , and
3. the total cross section of electrons for Compton scattering.

The results of the energy measurements will be compared with the predictions of Compton kinematics. The results of the scattering rate and cross section measurements will be compared with the predictions of the classical (Thomson) theory of X-ray scattering and with the Klein-Nishina formula derived from relativistic quantum theory.

The experimental setup employs a radioactive source of 661.6 keV photons from ^{137}Cs , and two NaI scintillation counters. One counter serves as the scattering target and measures the energy of the recoil electrons; the other counter detects the scattered photons and measures the energy they deposit. Both the target and scatter counters have a scintillator consisting of a $2'' \times 2''$ cylinder of Thallium-activated sodium iodide optically coupled to a photomultiplier. A 661.6 keV photon traversing sodium iodide has about equal probability of undergoing photoelectric absorption and Compton scattering. A photoelectric absorption event is a quantum mechanical transition from an initial state consisting of an incident photon of energy E and a neutral atom to a final state. This event therefore consists of an excited ion with a vacancy in one of its inner shells where the electron that was formerly bound and a free “photoelectron” with kinetic energy $E - W$, where W is the binding energy of the electron in the neutral atom. The energetic photoelectron loses its energy within a small fraction of a microsecond by multiple Coulomb interactions with electrons and nuclei in the sodium iodide crystal, and a certain fraction of the lost energy is converted into scintillation light. Meanwhile, the ion from which the photoelectron was ejected loses its energy of excitation through a cascade of transitions that fill the vacancy in its electronic structure and give rise to lower energy photons or electrons that, in turn, lose their energy in the crystal and generate additional scintillation light.

The total amount of scintillation light produced is closely proportional to the total amount of energy dissipated in all these processes. As a consequence, the pulse height spectrum of a NaI scintillation counter exposed to monoenergetic gamma rays shows a distinct “photoelectric” peak which facilitates accurate calibration in terms of pulse height versus energy deposited. The counters can then be used to measure the energies of scattered photons and recoil electrons. The following background topics should be studied in [2, 6]:

1. Kinematics and theory of Compton scattering;
2. Properties of ^{137}Cs ;
3. Scintillation counters and the interpretation of pulse height spectra (see preparatory question 3);
4. Radiation safety;
5. Parameter and error estimation [6].

II. EXPERIMENTAL ARRANGEMENT

The experimental arrangement for the Compton experiment is shown schematically in Figure 1. The $2'' \times 2''$ cylindrical “recoil electron” or “target” scintillator detector (Canberra model 802-3/2007), is irradiated by a beam of 661.6 keV photons emitted by about 100 μCi (≈ 1 microgram!) of ^{137}Cs located at the end of a hole in a large lead brick which acts as a gamma-ray “howitzer”. If a photon entering the target scintillator scatters from a loosely bound, effectively free, electron, the resulting recoil electron may lose all of its energy in the target, causing a scintillation pulse with an amplitude proportional to the energy of the recoil electron. If the scattered photon emerges from the target scintillator without further interaction, and if its trajectory passes through the NaI crystal of the “scattered photon” detector, it will have a substantial probability of depositing all of its energy by a single photoelectric interaction or by a sequence of Compton scatterings and photoelectric interactions. This will produce a scintillation pulse that contributes to the “photopeak” of the pulse height spectrum. The median channel of the photopeak in the multichannel analyzer (MCA) display is a good measure of the median energy of the detected photons. If the scattered photon undergoes a Compton scattering in the scatter scintillator and then escapes from the scintillator, the resulting pulse, with a size proportional to the energy of the Compton recoil electron, will be registered in the *Compton recoil continuum* of the spectrum. Several experimental details are considered in [7–11].

In the experimental arrangement described by [2] (pg. 256) the target is inert material (not a detector). The scatter counter suffers background due to gamma-ray photons leaking through the lead from the ^{137}Cs source, cosmic rays, and radioactive isotopes in the environment which is suppressed by the use of very heavy (≈ 200 lb) lead shielding around the source and the scatter counter. Without such shielding and without any electronic tricks the pulses produced by Compton scattered photons would be buried in the background. In a better way, the Compton scattered signal can be discriminated from the background using time coincidence techniques, as described in the following paragraphs.

In our experiment (see Fig. 1) both the recoil electron detector and the scattered photon detector are scintillation detectors. Circuits are arranged so that a pulse

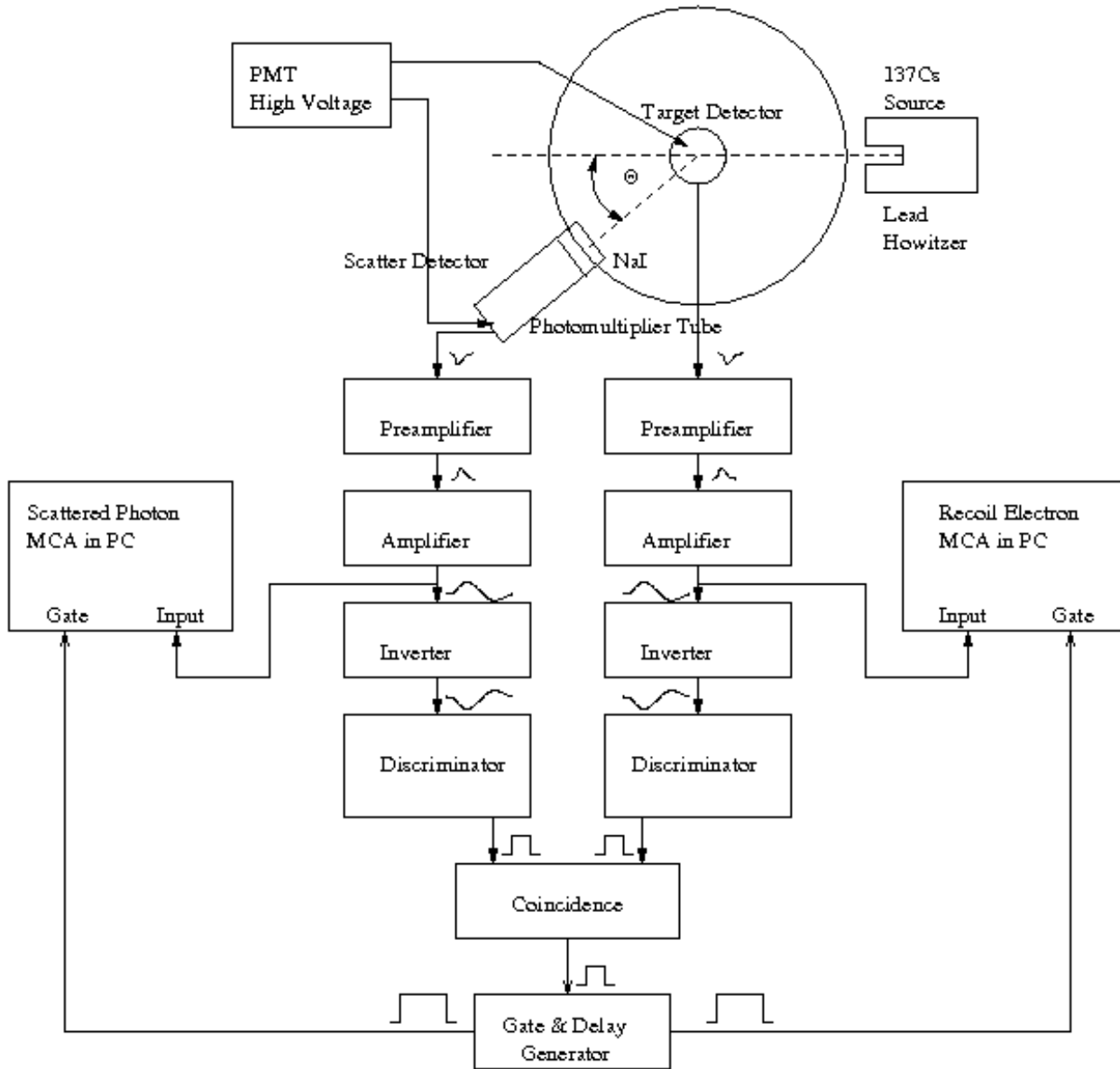


FIG. 1. Schematic diagram of the experimental arrangement for measuring Compton Scattering.

from a detector is accepted for pulse height analysis by the multichannel analyzer (MCA) only if it is coincident (within a fraction of a microsecond) with a pulse from the other detector. Coincident pulses occur when a gamma ray photon produces a Compton-recoil electron in the recoil electron detector, and the Compton-scattered photon is subsequently absorbed in the scattered photon detector. The two nearly simultaneous pulses produced in such an event are amplified and fed through inverters (Ortec model 533) to constant fraction discriminators (CFDs) (Canberra model 2126) whose threshold is user selectable between -50 mV and -1 V through a 10-turn potentiome-

ter. (The inverters are required because the amplifiers are designed to put out positive pulses, whereas the CFDs are designed for negative input pulses.) CFDs employ a historically interesting method to achieve precise timing described in Appendix B. Your experiment does not require this accuracy, and it is superseded by modern electronics.

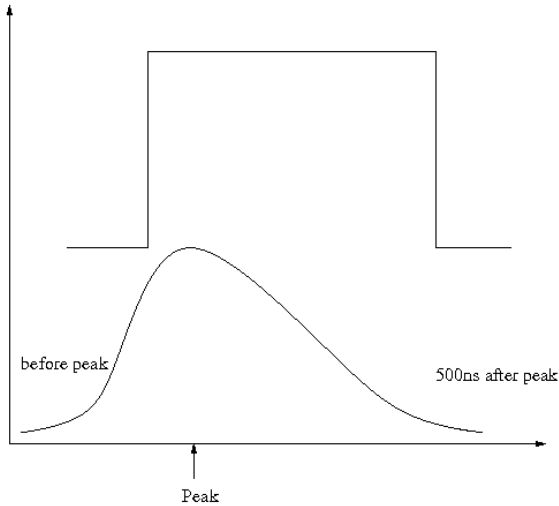


FIG. 2. Schematic representation of the proper time relation between the photomultiplier tube signal (amplified and inverted), whose pulse height is to be measured, and the coincident gate pulse produced by the Gate and Delay Generator NIM module. The coincident gate pulse needs to arrive before the peak of the pulse and persist for $\geq 0.5 \mu\text{s}$ after the pulse peak.

II.1. Coincidence Techniques

A true Compton event will produce coincident (within $2 \mu\text{s}$) signals in both detectors. If the logic (square) discriminator outputs overlap, the coincidence (‘AND’) produces an output ‘YES’ signal to the gate generator, which in turn notifies the MCA in the computer to analyze the pulse heights generated by this event. Most likely it is a ‘Compton event’, however there is a chance that two different background events accidentally occurred within the overlap time 2τ given by the discriminator outputs. From a scatter counter with rate n_s and target counter with rate n_t the accidental rate

$$n_{acc} = 2\tau n_s n_t \quad (2)$$

is small unless you have noise increasing n_s or n_t . A good method to set up the coincidence uses a ^{22}Na source placed in between the two detectors. But for Compton coincidences, consider that for small θ , the recoil (target) energy and hence signal are small. If the signals are below your discriminator threshold, you fail to see coincident Compton events at small θ .

II.2. Gating the MCA

In principle, the gate should tell the MCA ‘ahead of time’ that a good event is coming. With the present electronics, this is not possible so we try to catch the majority of the signal (see Fig. 2) including the peak. The

analog pulse shown is derived from the ‘unipolar’ output of the amplifier. The ‘bipolar’ has positive and negative peaks and is more tricky to use. Nuclear physicists use it at high counting rates.

When you think you have everything working correctly, and before you commit to a long series of measurements, check the performance at the extreme values of θ , say 0° and 150° . At both positions the peaks in the spectra due to the scattered photons and the recoil electrons should stand out clearly. If they do not, then more adjustments must be made to achieve correct operation of the coincidence gate logic. In coincidence mode, the MCA histogram is not updated unless an appropriate gate pulse arrives at the gate input during the rise of the signal pulse. During the “dead time” required for each pulse height analysis ($\approx 8 \mu\text{s}$ for the MCAs used in Junior Lab) the input to the pulse height analyzer is held closed by a “disable gate” so that the arrival of a second pulse will not interfere with the current analysis. More details of the specific MCAs (Perkin-Elmer model Trump-PCI) used in Junior Lab are available in the Junior Lab Filing Cabinet or in the online e-library.

III. EXPERIMENTAL PROCEDURE

Keep the lead door of the gamma-ray howitzer closed when not in use. The purpose of the procedures described below is to acquaint you with the operation of the equipment, particularly the coincidence scheme which permits the experiment to achieve a good signal/background ratio with a minimum amount of shielding. The steps below suggest a sequence of tests and adjustments to achieve that purpose, but you should feel free to devise your own.

III.1. Experimental Calibration

Set up and test the experimental arrangement with 511 keV annihilation photons from a ^{22}Na calibration source. ^{22}Na , a radioactive isotope of sodium, decays to an excited state of ^{22}Ne by emission of an anti-electron, *i.e.* a positron. The excited neon nucleus, in turn, decays quickly to its ground state by emission of a 1.27 MeV photon. Meanwhile, the positron comes to rest in the material in which the sodium isotope is embedded, combines with an electron to form an electrically neutral electronic atom called positronium (discovered in 1947 by Prof. Martin Deutsch of MIT). The latter lives about 10^{-7} s until the electron and positron annihilate yielding two 511 keV ($= m_e c^2$) photons traveling in opposite directions. Thus ^{22}Na is a handy source of pairs of monoenergetic photons traveling in opposite directions which can be used to test a coincidence detector system.

1. Set up the NaI recoil electron and scattered photon scintillation detectors as illustrated in Figure

1. Turn on the power to the NIM bin, HV supplies, MCA and oscilloscope. Keep the door on the ^{137}Cs source howitzer closed to reduce the intensity of 661.6 keV photons at the detectors.
2. Adjust the gain of the scattered photon detector and calibrate it. Apply high voltage to the scatter counter photomultiplier ($\approx +1000$ VDC). Using the MAESTRO-32 MCA software, turn off the coincidence gate requirement on the MCA. Place the ^{22}Na calibration source near the scattered photon detector and examine the output of the scattered photon amplifier signal (following the pre-amplifier AND the amplifier in series) with the oscilloscope. Adjust the gain so that the amplitude of the pulses produced by 511 keV annihilation gamma rays is about +7 volts. (You might see that a few very high energy pulses saturate the amplifier resulting in 'square' peaked signals. Since the Compton scattering experiment will measure only energies < 661.6 keV, it is okay to discriminate against these pulses.) Determine the gain setting of the primary amplifier at which non-linear response begins, as indicated by a flattening of the top of the pulse as viewed on the oscilloscope. Then reduce the primary amplifier gain sufficiently to assure a linear response up to energies safely above the 661.6 keV energy of the ^{137}Cs photons.

Now feed the output pulses from the amplifier to the input of the MCA and acquire about 30 seconds of pulse height data using the acquisition presets sub-menu. Examine the Energy spectrum/histogram of pulses from the scattered photon detector and adjust the gain of the amplifier so that the median channel of the photopeak for 511 keV photons is $\approx 2/3$ of the full scale MCA range (check that this is set to 2048 channels). Calibrate the counter with other plastic rod calibration gamma-ray sources. A good set consists of ^{137}Cs (661.6 keV), ^{22}Na (511 keV), and ^{133}Ba (356, 302, and 81 keV plus other lines) each of which produce easily identified photopeaks. Be aware that too high a counting rate will spoil the spectrum by overlapping signals and amplifier saturation.

Write in your lab notebook a succinct description of what you are doing along with the data so that you can later recall exactly what you did and repeat it quickly. You will have to redo the calibration at the start of each lab session because other users will have changed the settings. When you have identified the photopeaks and are confident about the counting rates, measure the median channels of the photopeaks and plot the average median photopeak channel numbers versus the photon energies on millimeter graph paper to provide yourself with a calibration curve. The simplest way to estimate the random error in a measurement of the median is to

repeat it five or more times and then evaluate the root mean square (RMS) deviation of the successive measurements from their mean value.

3. Adjust and calibrate the recoil electron 'target' detector in the same way.
4. Send the amplified recoil electron and scattered photon signals to the Inverter module and then send the resultant negative polarity pulses into the two discriminators. Examine the positive output pulses generated by the units.
5. Send the two discriminator outputs into channels 1 and 2 of the coincidence module and examine its output. (It is easiest if you temporarily use a single detector signal to trigger both discriminators for this test.)
6. Send the output from the coincidence circuit into the gate generator unit and explore its operation. Adjust the delay of the delay amplifier so the coincidence gate pulse arrives at the MCA gate input during the rise of the analog signal pulse (see Figure 2). A good way to verify the action of the gate pulse is to feed the pulses from one of the amplifiers to both CFD inputs. This will ensure that a coincidence pulse is generated at relatively high rates. (Students should play with the gate generator controls, specifically delay and width, to verify the operation of the MCA card coincidence circuitry as described in Figure 2.)
7. Test the coincidence logic. Place the ^{22}Na source between the two scintillators so that pairs of annihilation photons traveling in precisely opposite directions can produce coincident pulses in the two counters. For this test it is interesting to reduce the gain by a factor of 2 so that the photopeak of the 1.27 MeV photons can be seen on the MCA spectrum display. Compare the spectrum with and without the coincidence requirement, and observe the effect of moving the source in and out of the straight line between the scintillators in order to observe hits by a pair of annihilation photons. Take careful notes and be sure you understand what you observe. Do not hesitate to ask for help if you need it. **In each of the above steps it is very useful to sketch a picture (or generate a bitmap using the Agilent digital oscilloscopes) of the waveforms taking particular note of their amplitudes, rise and fall times and temporal relationships with other signals, e.g. gates.**

III.2. Compton Scattering Using ^{137}Cs

This section details the measurement of the energies of the scattered gamma rays and the recoil electrons as functions of the scattering angle θ .

1. Align the primary gamma-ray beam from the ^{137}Cs source in the howitzer. Position the howitzer and the scatter counter so that the source (at the inside of the hole in the lead howitzer) and the scatter counter scintillator are at opposite ends of a diameter of the round platform, with the source ≈ 40 cm from the center of the scintillator. (Keep careful notes about the exact geometry you choose for the setup so you can return to it if necessary at a later time.) Open the door of the howitzer and measure the rate of pulses in the photopeak from the scatter counter as a function of its position angle. In other words, measure the “profile” of the beam and determine $\theta = 0$. Check that the beam profile is symmetric about a line from the source through the center of the turntable to insure that the target counter will be uniformly illuminated when it is placed at the center.
2. Adjust the discriminators of the CFDs to insure that they will generate coincident pulses whenever a Compton scattering occurs in the target scintillator with a scattering angle in the range you wish to cover. Position the NaI target counter over the center of the turntable at a height such that the axis of the beam intersects the mid-plane of the scintillator. For a preliminary test, connect the (inverted) output of the target amplifier to the inputs of both CFDs. Simultaneously connect the output of the target amplifier to the INPUT BNC connector on the MCA card in the PC. Connect the output of the coincidence circuit to the gate generator module and the output of the gate generator to the GATE BNC on the MCA card. Using the MAESTRO-32 software package, set the discriminators as low as possible without getting into the rapidly rising spectrum of photomultiplier noise such that the accidental coincidence rate would rival the true coincidence rate. Start a spectrum accumulation and test the effects of changing the delay of the gate pulse with respect to the signal pulse.
3. **Measure the median energy E'_γ of scattered photons and the median energy E_e of recoil electrons as functions of the position angle θ' of the scattered photon detector.** With both the source in the howitzer and the scintillator of the scattered photon detector located ≈ 40 cm from the recoil electron detector, set the position angle of the scatter counter at 90° . With the coincidence requirement enabled, accumulate a spectrum of scattered photon detector pulses on the ‘scatter’ MCA and a spectrum of recoil electron detector pulses on the ‘target’ MCA and measure the median channel of the pulses in the photoelectric peaks. Repeat this dual measurement at several position angles from just outside the primary beam profile to as near to 180° as you can get. A good strategy is to take data at widely separated position angles, say

90° , 30° , 120° , 150° and then fill in when you have time. Plot the raw results (median energy against position angle) as you go along to guide your measurement strategy. It is wise to check the calibration between each measurement by switching the (software based) gate setting to ‘OFF’ and recording in your notebook the median channels of the photopeaks produced by 661.6 keV photons from the ^{137}Cs calibration source, the 511 keV photons from ^{22}Na , and the 356 keV and 81 keV photons of ^{133}Ba .

Record the integration time of each measurement to find the rate as a function of θ to later compare with Thomson’s classical prediction.

III.3. Scattering Cross Section Measurements

In this part of the experiment, you will measure the total scattering cross section per electron in plastic. The plastic scintillator blocks used as absorbers in this measurement are made from polyvinyltoluene ($\text{C}_{10}\text{H}_{11}$, density 1.032 g/cm^3 , www.bicron.com) composed of almost equal numbers of carbon and hydrogen atoms. The most tightly bound electrons are in the K-shells of the carbon atoms where they are bound by 0.277 keV, which is small compared to 661.6 keV. In fact, many other materials can be used providing approximately ‘free’ electrons. This material resembles most modern plastic scintillators. You will determine their quantum efficiency, *e.g.* how often they ‘see’ γ -rays. Place the scatter counter at 0° and remove the target counter from the beam. Measure the counting rates in the 661.6 keV photopeak of the NaI scatter counter with no absorber and with three or more different thicknesses of plastic scintillator placed just in front of the exit hole of the howitzer. Determine the thicknesses (in g/cm^2) of the scintillator blocks by measuring their dimensions and mass. Plot the natural logarithm of the measured rate as a function of the thickness and check the validity of your data by observing whether the data points fall along a straight line as expected for exponential attenuation. Question: Why is it better to place the absorbers as near as possible to the source rather than just in front of the detector?

IV. ANALYSIS

1. Plot $E_{\text{target}} + E_{\text{scatter}}$ vs. θ .
2. Compare your results on the angular dependence of energies of the scattered photons and the recoil electrons with the predictions of the Compton formula. Since the relation between the scattered photon energy E'_γ and the scattering angle θ , is non-linear, one can anticipate that a plot of the

measured energy versus position angle could be fitted only by a curve. However, an easy manipulation of the Compton formula yields a linear relation between $1/E'_\gamma$ and $1 - \cos\theta$. Plot $1/E'_\gamma$ against $(1 - \cos\theta)$ with appropriate error estimates. On the same graph plot the calculated curve of $1/E'_\gamma$ against $(1 - \cos\theta)$ based on the Compton formula. Do a similar analysis of the recoil electron data on a separate graph. Plot $1/E_e$ against a function of θ such that the expected relation is linear. Comment on the degree of conformance of the prediction to your experimental results and discuss possible causes of any systematic differences.

3. Plot the measured 'rate' as a function of θ and compare to the classical Thomson prediction.
4. Compute the total interaction cross section per electron. The attenuation of a collimated beam of particles by interactions in a slab of material of thickness x (in centimeters) is described by the formula

$$I(x) = I_0 e^{-\mu x}, \quad (3)$$

where I_0 is the initial intensity and μ is the total linear attenuation coefficient (cm^{-1}). In plastic scintillator the attenuation of 661.6 keV photons is due almost entirely to Compton scattering. Under this circumstance the total attenuation coefficient

is related to the Compton scattering cross section per electron, which we call σ_{total} , by the equation

$$\sigma_{total} = \frac{\mu}{n_e}, \quad (4)$$

where n_e is the number of electrons/ cm^3 of the material. To find μ from your data, you should fit an exponential directly to the data, determining the best-fit parameters and their errors. Alternatively, you may plot the natural log of the measured values of I/I_0 against x . Then determine the slope (and its error) of the straight line that best fits the data by linear regression. In either case, calculate the number of electrons/ cm^3 of scintillator $(CH)_n$, and find σ_{total} . Compare to the classical Thomson calculation and to the theoretical result of Klein-Nishina [12].

IV.1. Suggested Theoretical Topics

1. Relativistic mechanics and the Compton shift.
2. Derivation of the Thomson differential and total cross section for unpolarized photons.
3. Discuss the 'correct' Klein-Nishina prediction.

-
- [1] A. Compton, Phys. Rev. **21**, 483 (1923), brother of K.T. Compton, MIT President.
 - [2] A. Melissinos and J. Napolitano, *Experiments in Modern Physics*, 2nd ed. (Academic Press, Orlando, 2003).
 - [3] A. Compton, Phys. Rev. **22**, 409 (1923).
 - [4] A. Compton, Nobel Prize Lecture(1927).
 - [5] A. Compton and S. Allison, *X-Rays in Theory and Experiment* (Van Nostrand, Princeton, 1992) qA481.C738 Physics Department Reading Room.
 - [6] P. Bevington and D. Robinson, *Data Reduction and Error Analysis for the Physical Sciences*, 3rd ed. (McGraw-Hill, 2003).
 - [7] G. Knoll, *Radiation Detection and Measurement*, 3rd ed. (John Wiley, Orlando, 1999) ISBN 0471073385.
 - [8] R. D. N.H. Lazar and P. Bell, Nucleonics **14**, 52 (1956).
 - [9] R. Garner and K. Verghese, Nuclear Instruments and Methods **93**, 163 (1971).
 - [10] R. Hofstadter and J. McIntyre, Physical Review **78**, 619 (1950).
 - [11] J. Higbie, American Journal of Physics **42**, 642 (1974).
 - [12] D. J. Griffiths, *Introduction to Quantum Mechanics* (Prentice-Hall, 1995).

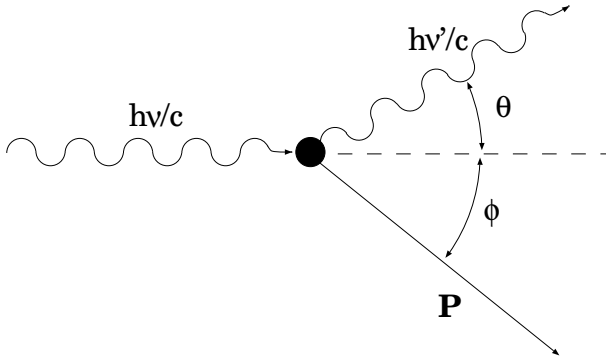


FIG. 3. Schematic representation of Compton scattering.

Appendix A: Derivation of the Compton Scattering Formula

Consider the interaction between a photon with momentum vector \mathbf{p}_γ (and zero rest mass) and an electron initially at rest with rest mass m_e as depicted in Figure 3. Call \mathbf{p}'_γ and \mathbf{p}'_e the momenta of the photon and the electron after the interaction, respectively. By conservation of momentum, the relation between the initial and final momenta is

$$\mathbf{p}_\gamma = \mathbf{p}'_\gamma + \mathbf{p}'_e. \quad (\text{A1})$$

Rearranging and squaring both sides we obtain

$$p_\gamma^2 + p_e'^2 - 2\mathbf{p}_\gamma \cdot \mathbf{p}'_e = p_e'^2. \quad (\text{A2})$$

The total relativistic energy E and momentum \mathbf{p} of a particle are related to its rest mass m by the invariant relation $(\mathbf{p} \cdot \mathbf{p})c^2 - E^2 = -m^2c^4$. By conservation of energy,

$$p_\gamma + m_e c = p'_\gamma + \sqrt{m_e^2 c^2 + p_e'^2}. \quad (\text{A3})$$

Rearranging and squaring both sides, we obtain

$$p_\gamma^2 + p_e'^2 - 2p_\gamma p'_\gamma + 2m_e c(p_\gamma - p'_\gamma) + m_e^2 c^2 = m_e^2 c^2 + p_e'^2. \quad (\text{A4})$$

Subtraction of Equation (A2) from Equation (A4) and rearrangement yields

$$m_e c(p_\gamma - p'_\gamma) = p_\gamma p'_\gamma - \mathbf{p}_\gamma \cdot \mathbf{p}'_\gamma. \quad (\text{A5})$$

Finally, dividing both sides by $m_e c p_\gamma p'_\gamma$, we obtain for the relation between the energies of the incident and the scattered photons the equation

$$\frac{1}{E'_\gamma} - \frac{1}{E_\gamma} = \frac{1}{m_e c^2} (1 - \cos \theta), \quad (\text{A6})$$

where θ is the angle between their final momentum vectors.

Appendix B: Introduction to Timing

A timing instrument marks or measures the precise occurrence of nuclear events. In practice, the release of electrons, which result from the detector's absorption of a particle's energy, occurs after the actual event; how long after is dependent upon the detector and how it is employed. The electronics processing this output further modifies its characteristics. All of these factors must be accounted for, in addition to the problem of noise, when making precise and highly resolved timing measurements.

Sharp timing (2τ overlap) reduces the number of 'accidentals'. The primary limitations in this (and other) experiments is the time slew. A pulse of lower amplitude reaches the threshold of the discriminator later. The coincidence time has to be enlarged to ensure overlap with the other 'normal' (earlier) signal. The time slew is large because the rise time our amplifiers is 'slow'. To overcome timing inaccuracies from 'slew' and differing pulse shapes, the constant fraction technique is used.

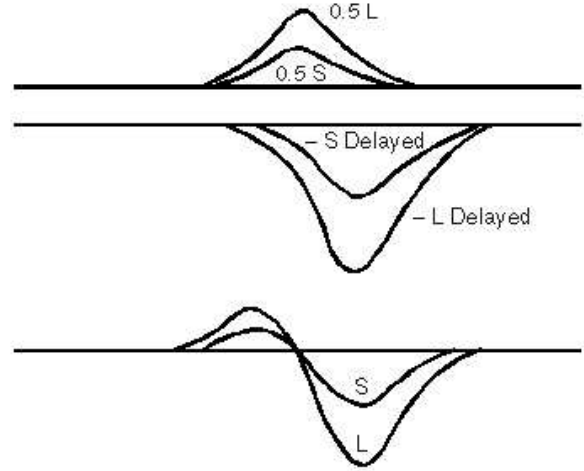


FIG. 4. Manipulation of input signal for constant fraction discrimination.

Constant fraction timing involves the inversion, delay and recombination of the signal to create a zero crossing mark. However, rather than adding the inverted and delayed signal to the original to achieve cancellation, some fractional part of the original is used to insure baseline crossover. As is evident in Figure 4, the crossover point is independent of amplitude of the input signal. The constant fraction discriminator (CFD) fixes its reference at this point.

1. Constant Fraction Discrimination

CFDs have an advantage over simple discriminators in experiments that require the detection of coincidences with high time resolution. A simple discriminator produces a logic output pulse that starts at some fixed time

after the voltage at the input rises above a set value. Therefore pulses of similar shape but different peak amplitudes trigger a simple discriminator at different times relative to the occurrence times of the events that generate the input pulses. A CFD also produces a logic output pulse if the voltage of the input pulse exceeds a set value; its special virtue is that the output pulse starts at a fixed time after the input pulse has risen to a certain constant fraction of its peak value, independent of the magnitude of that peak value. If the input pulses have a fixed shape, but different amplitudes, then the delay between the event that produces the input pulse and the logic output pulse from the CFD will be a constant, which can be adjusted by the WALK control. The positive +5 VDC outputs of the CFDs are fed to a coincidence circuit that produces a logic pulse when all of its *enabled* input ports see pulses within the selected resolving time (user selectable within two ranges: “fast coincidence” 10–100 ns or “slow coincidence” 100–1000 ns). The output pulses from the coincidence circuit are fed to a gate generator and delay module, after which, the suitably stretched and delayed gate signal is sent to the GATE input of the MCA.

The amount of delay and the gate width in the delay module should be adjusted to meet the requirements of the coincident gate mode of the MCA. This requirement is that the gate pulse begin before the peak of the analog input signal and last for at least $0.5 \mu\text{s}$ beyond the peak. The coincidence gate requirement suppresses background events and makes the Compton scatter events stand out clearly in the resulting pulse height spectrum without the use of heavy shielding.

Appendix C: Scintillation Counter Efficiency Calculations

A significant complication in the analysis of the data on the differential cross section is the fact that the target is not “thin”, *i.e.* the mean free paths of the incident and scattered photons suffer substantial attenuation as it passes through the target material, and the scattered photons suffer substantial attenuation in their passage out of the target. The effects of these attenuations on the counting rate obviously depend on the position of the detector. A count must therefore be taken of these thick target effects in order to derive accurate values of the differential cross section from the measured counting rates at various scattering angles.

As in all cross section measurements, the necessarily finite sizes of source, target and detector introduce into the analysis geometrical factors that require laborious multidimensional integrations for their evaluations. In our experiment we have a divergent beam of photons from a radioactive source of finite size that can interact at various depths in the target within certain ranges of solid angle to produce scattered photons that traverse the detector would be a convolution of the differential cross

section with geometrical and attenuation factors represented by a multiple integral over at least ten variables with hideous limits of integration. The only practical way around this kind of mess in particle physics experiments where the highest possible precision is required is the “Monte Carlo” technique in which the sequence of physical processes from emission to detection is sampled by use of appropriate distribution functions to represent the various possible processes, and random numbers to select the outcome of each process.

Here we outline an approximate analytical treatment of our problem based on several simplifying assumptions. The formulation is suitable for numerical computation on a modest computer. We will consider only single scattering events. We call R and H the radius and length, respectively, of the cylindrical scintillators which are the sensitive elements of the target and scatter counters. We assume that the source is so far from the target scintillator that the incident beam may be considered uniform and parallel (*i.e.* unidirectional). We assume that the distance D of the scatter counter scintillator from the target is so large that the detected portion of the scattered radiation may be considered to comprise a parallel (but not uniform) beam.

Consider the scatterings that occur within a solid element of volume $r d\phi dr dz$ at a position in the target scintillator with cylindrical coordinates r , ϕ , z . As can be deduced with the aid of Figure 5, the distance x of this element from the point of entry of the incident photons into the target scintillator is given by the expression

$$x = R\{[1 - (q \sin \phi)^2]^{\frac{1}{2}} - q \cos \phi\}, \quad (\text{C1})$$

where $q = r/R$. Similarly, for photons scattered from the point P at the angle θ , the distance y of the element from the point of exit is

$$y = R\{[1 - (q \sin \psi)^2]^{\frac{1}{2}} - q \cos \psi\}, \quad (\text{C2})$$

where $\psi = \pi - \theta + \phi$. We call α the total linear at-

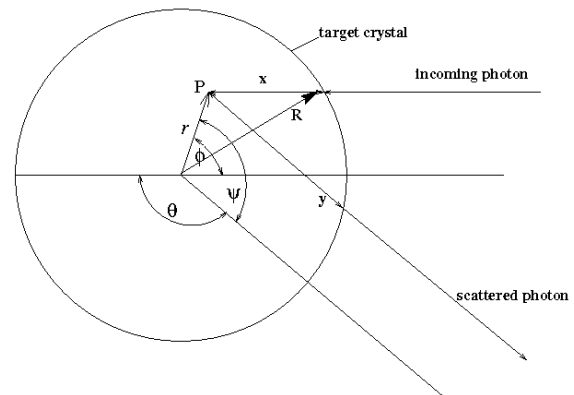


FIG. 5. Diagram of the Compton scattering geometry.

tenuation coefficient (units of cm^{-1}) of the target plastic

scintillator for the incident photons, $\beta(\theta)$ the total linear attenuation coefficient of the plastic for photons scattered at angle θ , and $\gamma(\theta)$ the total linear attenuation coefficient of the scatter counter NaI scintillator for those scattered photons. The efficiency for detection of scattering events that occur at a given position in the target scintillator is $\exp(-\beta y)[1 - \exp(-\gamma H)]$ which represents the probability that the scattered photon will escape from the target counter multiplied by the probability that the scattered photon interacts in the scatter counter.

We must now find the average of this efficiency over the target scintillator. Recalling the assumption that the incident beam is parallel and uniform, the weighting factor is $I_0 \exp(-\alpha x)$ which is the intensity of the incident beam at the point of interaction inside the target scintillator. We can now write for the average efficiency the expression

$$\eta(\theta) = \frac{\int \exp(-\alpha x) \exp(-\beta y) [1 - \exp(-\gamma H)] dV}{\int \exp(-\alpha x) dV}, \quad (\text{C3})$$

where the integrals are computed over the volume of the target scintillator. We note that $\eta \rightarrow 1$ as $\alpha \rightarrow 0$, $\beta \rightarrow 0$.

The total attenuation coefficients are functions of the energy of the scattered photon and the energy of the scattered photon is a function of the scattering angle. According to the Compton theory,

$$E_\gamma(\theta) = \frac{E_0}{1 + (E_0/mc^2)(1 - \cos \theta)}. \quad (\text{C4})$$

In the energy range from 0.2 MeV to 0.7 MeV, the total attenuation coefficient in sodium iodide can be fairly represented by the formula

$$\mu = \left[0.514 \left(\frac{E}{100 \text{ keV}} \right)^{-0.368} + 5.51 \left(\frac{E}{100 \text{ keV}} \right)^{-2.78} \right] \text{ cm}^{-1}, \quad (\text{C5})$$

and in plastic by the formula

$$\mu = 0.177 \left(\frac{E}{100 \text{ keV}} \right)^{-0.37} \text{ cm}^{-1}. \quad (\text{C6})$$

The quantity η can be evaluated as a function of θ by numerical integration.

MIT
OpenCourseWare
<https://ocw.mit.edu>

8.13-14 Experimental Physics I & II "Junior Lab"
Fall 2016 - Spring 2017

For information about citing these materials or our Terms of Use, visit: <https://ocw.mit.edu/terms>.